

## Heavy minerals: from ‘Edelstein’ to Einstein

R.J. de Meijer \*

*Environmental Radioactivity Research and Consultancy Group, Kernfysisch Versneller Instituut, Rijksuniversiteit Groningen,  
Zernikelaan 25, 9747 AA Groningen, Netherlands*

Accepted 6 November 1997

---

### Abstract

Identification in 1982 on the Dutch Frisian Island of Ameland of beach sand with an enhanced level of natural radioactivity, due to concentrations of heavy minerals, inspired a multi-disciplinary research project. A joint research effort in geochemistry, sedimentology, hydrodynamics, solid-state physics and nuclear physics has revealed new aspects in the use of natural radioactivity in heavy-mineral exploration and processing, as well as in understanding sediment transport processes in the coastal zone. This paper describes radiometric methods and techniques, such as thermoluminescence dating and a method known as radiometric fingerprinting. Initially our focus was on relationships between natural radioactivity and grain size, and between radioactivity and mineral species. Additionally the distribution of heavy minerals along the Dutch coast was mapped. One of the first substantial findings was that the concentrations of K, U and Th in light and heavy minerals differ by two orders of magnitude. Thus the total heavy-mineral mass fraction (THM) could be accurately determined radiometrically. Attempts to determine THM radiometrically resulted in identifying regions of provenance, or origin for coastal sand minerals. This stimulated studies of transport processes and their selectivity. Investigations were conducted on the beach, under laboratory conditions and on the seafloor. Moreover, the enhanced radionuclide concentrations in, e.g., zircons make them particularly suitable for thermoluminescence dating young dune and beach sediments. This knowledge may aid better management of coastal zones, and may help to identify the genesis conditions of heavy-mineral placers. The instrumentation development has resulted in MEDUSA a towed detector system used for radiometric seafloor mapping. MEDUSA revealed unknown large quantities of heavy minerals on the Dutch seafloor. These minerals are present in layers up to 40% in thickness and with concentrations up to 20%. Radiometric fingerprinting of minerals allows a quantitative assessment of mineral suites during various stages of wet and dry separation. This industrial application of MEDUSA is being considered in Australia and South Africa. © 1998 Elsevier Science B.V. All rights reserved.

*Keywords:* natural radioactivity; heavy minerals; exploration; processing; sediment transport; sediment dynamics

---

### 1. Introduction

Minerals are naturally occurring crystalline inorganic substances. Mineral sediments—sand and mud—are weathered from mountain belts, transported by

rivers, glaciers or wind and deposited at the coast or beyond. Heavy minerals are those minerals that are denser than bromoform (spec. dens.  $2.9 \text{ kg l}^{-1}$ ); light minerals will float on bromoform. Some of the heavy minerals such as diamonds, tourmaline and epidote are also known as gemstones (in German ‘Edelstein’).

---

\* E-mail: demeijer@kvi.nl

Minerals as crystals are orderly arrangements of atoms. Due to the arrangements, minerals have physical properties with a wide range of values. In addition to density, minerals vary strongly in electric conductivity and magnetic susceptibility. These and the more special properties of minerals are well used in separation of minerals in the mining industry. An example of the application of a special property is the X-ray fluorescence of diamonds. In one of the last stages of processing of offshore diamond mining operations, diamonds are separated from the other minerals by opening in time a valve on a slope over which the materials are sliding down. This valve is operated by a light sensor which detects the fluorescent light of diamonds.

This overview is limited to sands, defined as sediments with a diameter between 0.063 and 2.0 mm. Quartz and feldspar are light minerals that usually form the bulk of sand deposits. For most large-scale coastal regions, heavy minerals occur with mass percentages of 1% or less. Locally, however, concentrations may be considerably higher: up to several tens of percent.

These areas of higher concentration may be of economic interest if mass percentages of valuable heavy minerals in the deposit are large enough and if the volume of the deposit allows mining for a considerable time at low costs. Concentrations of heavy minerals also indicate selective transport processes, known to be dependent on grain size and density. Understanding this selectivity may help to more effectively search for economically valuable deposits, and also to better understand sediment transport in the coastal region and the mechanisms of accretion and erosion. Such understanding leads in turn to a better assessment of the environmental aspects of the heavy-mineral sand mining process.

Some of the heavy minerals such as zircon ( $\text{ZrSiO}_4$ ), rutile ( $\text{TiO}_2$ ) and ilmenite ( $\text{FeTiO}_3$ ) are predominantly mined from coastal placers, both modern and palaeo. They form the ore from which metals such as zirconium and titanium are extracted, both of which are sources of metals with a wide industrial application. Moreover, heavy minerals tend to incorporate higher concentrations of the naturally occurring radionuclides of the uranium and thorium decay series in their crystalline structure. Light minerals such as quartz and feldspar are low in uranium

and thorium, but especially feldspar may contain relatively high concentrations of K, which has an isotope ( $^{40}\text{K}$ ) which is a natural  $\gamma$ -ray emitter. Being radioactive, both light and heavy minerals emit characteristic  $\gamma$ -radiation. The concentration of these radionuclides is mineral-specific and therefore constitutes a radiometric fingerprint for the mineral. Due to these properties light and heavy minerals can be rather easily detected and the composition of their suite can be derived. Radiometric fingerprinting therefore can be a sensitive tool in sand transport studies, heavy-mineral exploration and mineral processing.

Besides  $\gamma$ -radiation,  $\alpha$ -radiation is present in the decay series of uranium and thorium. Due to the short range of  $\alpha$ -particles, almost all energy is released within the crystal that incorporates these radionuclides. Part of this energy is converted to electrons trapped in metastable states, created in the lattice by, e.g., trace elements. Exposure to (sun)light or heating of the crystal will release these trapped electrons and their surplus energy is partly emitted as visible light through the process of thermoluminescence (TL). The amount of light emitted is proportional to the stored energy, which is in turn proportional to exposure time and radiation dose rate. Because the TL signal in sediments on, e.g., a beach or a shallow seafloor is continuously reset by the exposure to sunlight, the amount of light emitted during heating is a measure of the time elapsed since burial.

Sediment transport is a complex problem to describe physically because sediment bed and fluid flow have strong interactions. In practice, workable approximations are employed to reduce the complex descriptions. With modern computer power, however, one is reasonably able to calculate from wind directions and coastal morphology the water velocity distribution in the coastal zone. One of the difficult problems remaining is the description of sediment transport. One of the many investigators who have worked on the description of these problems was Hans Einstein, son of the famous physicist Albert Einstein. Once the father, having a discussion with his son, told Hans that he was glad not to have to work with such complex problems as sediment transport!

This paper will discuss the application of heavy

minerals to understanding transport processes like bed-load transport, one of the topics of interest to Hans Einstein.

## 2. Radiometric properties of heavy minerals

The way trace elements are incorporated in crystals depends on the properties of the mineral, the stage at which they are formed in the cooling process and the abundance of these trace elements in the parent magma. If  $^{40}\text{K}$ ,  $^{238}\text{U}$  or  $^{232}\text{Th}$  are incorporated, the crystals become radioactive and the associated  $\gamma$ -rays may be detected. Elements like U and Th are the start of long decay series, finally ending up in stable Pb isotopes. One of the elements formed during the decay is the noble gas radon (Rn), which may escape from the crystal. The relatively long half-life time of  $^{222}\text{Rn}$  ( $^{238}\text{U}$  decay series) allows part of the radon to escape. Because the  $\gamma$ -rays are emitted by  $^{214}\text{Bi}$ , a decay product of the remaining  $^{222}\text{Rn}$  in the crystal, in this paper  $^{214}\text{Bi}$  is used to refer to  $^{238}\text{U}$ .

The results presented in this paper are derived from radiometric measurements and hence are expressed as activity concentrations ( $\text{Bq kg}^{-1}$ ); 1 Bq corresponds to one decaying atom per second. One ppm eU and eTh correspond to 12.3 and 4.0  $\text{Bq kg}^{-1}$ , respectively; 1%  $\text{K}_2\text{O}$  to 257  $\text{Bq kg}^{-1}$  of  $^{40}\text{K}$ .

Fig. 1 (de Meijer et al., 1985) shows, as a function of grain-size interval, the total activity and the activity concentrations of  $^{214}\text{Bi}$  (indicated as  $^{222}\text{Rn}$ ),  $^{232}\text{Th}$  and  $^{40}\text{K}$  for three sand samples taken on the beach of Ameland, in the Dutch Frisian Islands; the location along the beach is indicated by the number of the beach pole. From this figure one notices that the activity concentrations for a given grain-size interval is almost independent of the sample. Contrary to the  $^{40}\text{K}$  activity concentration, which varies only slightly with grain size, both the Bi and Th concentrations increase exponentially with decreasing grain size  $\phi$ : about three orders of magnitude when going from  $250 < \phi < 300 \mu\text{m}$  to  $\phi < 90 \mu\text{m}$ .

Fig. 2 (de Meijer et al., 1985) shows for one grain-size interval the concentrations of  $^{214}\text{Bi}$  and  $^{232}\text{Th}$  as function of magnetic susceptibility<sup>1</sup>, denoted by the magnet current I of a standard Frantz

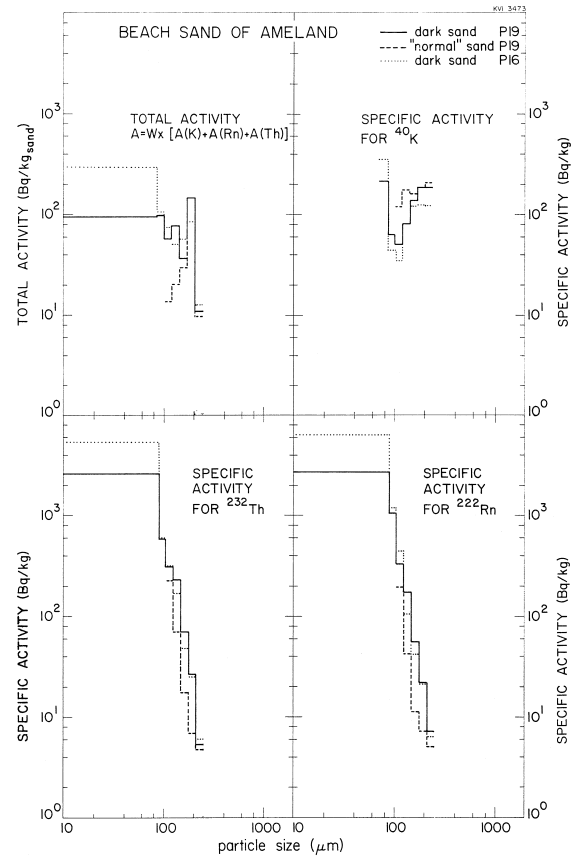


Fig. 1. Total and specific activity concentrations for three samples of beach sand taken on the beach of the Dutch Frisian Island of Ameland. The total activity is obtained by multiplying the relative weight of the fraction  $W$  by the sum of the specific activities  $A$ . Taken from de Meijer et al. (1985).

magnetic separator. The activity concentrations vary over about two orders of magnitude. The best separation of the Bi and Th activities occurs at the current intervals  $0.6 < I < 1.0 \text{ A}$  and  $I > 1.55 \text{ A}$ . These fractions contain mainly rutile (with some monazite ((Ce,La,Nd,Pr,Th) $\text{PO}_4$ )) and zircon, respectively; minerals that are known to incorporate thorium and uranium in their crystal lattices. So the activity concentration of these fractions is governed by the host minerals, which have been separated on the basis of their magnetic properties.<sup>1</sup>

<sup>1</sup> Compared to the original figure the  $^{40}\text{K}$  activities are omitted, because the  $^{40}\text{K}$  activity was mistakenly interpreted and originated from a  $\gamma$ -ray of the decay of  $^{232}\text{Th}$ , which was energetically not distinguishable from the  $^{40}\text{K}$  line.

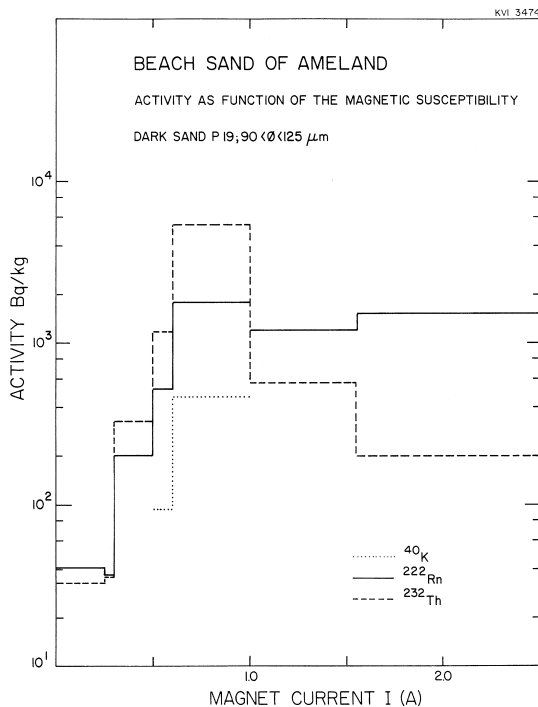


Fig. 2. Activity concentrations of  $^{214}\text{Bi}$  (denoted as  $^{222}\text{Rn}$ ) and  $^{232}\text{Th}$  (Bq kg) for various magnetic components of the fraction  $90 < \phi < 125\ \mu\text{m}$  from the dark sand at beach pole 19 (P19), separated in a Frantz separator. Taken from de Meijer et al. (1985).

For each mineral group the grain-size distribution was determined (Schuiling et al., 1985). Fig. 3 (de Meijer et al., 1985) shows the average grain size of each mineral group as a function of specific density. Except for magnetite, probably due to magnetic clustering, all values are more or less on a straight line, indicating that specific density is the dominant factor that determines which grain sizes of each mineral will be deposited side by side in the same sediment (i.e., grains of the same settling velocity). The deviations from a straight line are probably a result of the fact that the actual grains are not ideal spheres. This phenomenon, which occurs often in sediments is also called hydro-equivalence.

Fig. 4 (de Meijer et al., 1989) shows concentrations of various radioactive and stable elements obtained through XRF analysis. In this figure La is chosen to represent the rare-earth elements. The

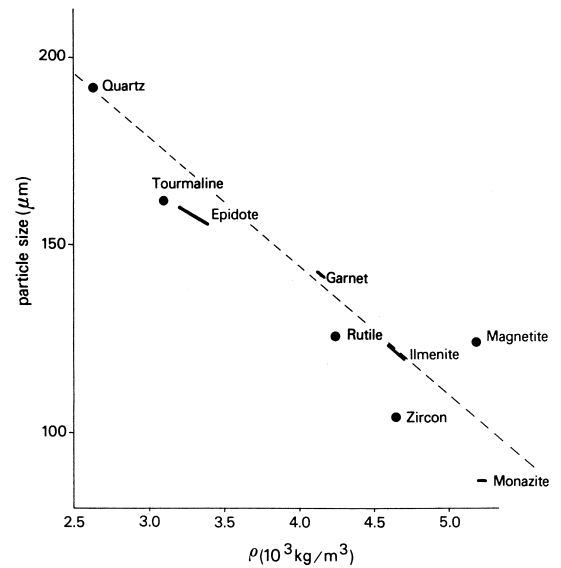


Fig. 3. Average grain sizes for various minerals as function of their specific density. Taken from de Meijer et al. (1985).

figure indicates that Zr dominates in the smaller fractions, pointing to the occurrence of the mineral zircon in the fine sand fraction and that K is mainly present in the larger grains, obviously indicating the occurrence of feldspar and possibly muscovite grains. Moreover one notices that U follows the distribution of Zr, and Th and La follow P, thus reflecting the

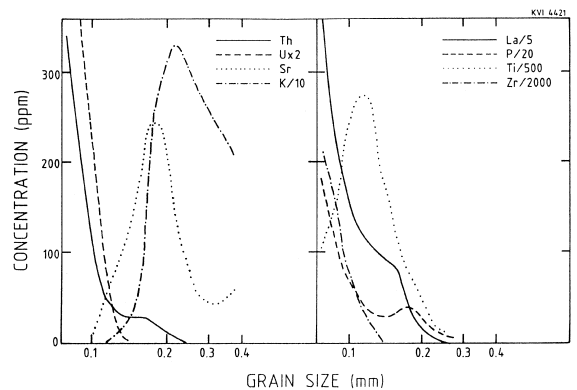


Fig. 4. Concentrations of various elements as determined by chemical analysis in the Ameland P19 sample. The multiplicative numbers indicate the factor by which the original concentration was multiplied ( $\times$ ) or divided ( $/$ ) to bring them to the scale indicated. Taken from de Meijer et al. (1989).

presence of zircon and monazite, respectively. The P anomaly near  $\phi = 0.2$  mm corresponds with the maximum of the Sr concentration, which suggests the presence of apatite (calcium phosphate).

A similar study in which a sample was split into a light and heavy fraction and the heavy fraction was separated according to magnetic susceptibility was carried out for samples taken at De Hors, Texel (NL) and Bergen (NL) (de Meijer et al., 1990) and again more recently at the west coast of South Africa (Macdonald et al., 1997). In both cases the activity concentration was found to depend considerably on the magnetic susceptibility. Since magnetic susceptibility reflects mineral properties, the result indicates that activity concentrations are mineral-specific. This indication could be proven by taking samples from the heavy-mineral industry.

In heavy-mineral processing various physical methods are utilised to obtain almost pure, single-species heavy-mineral groups. Table 1 lists the results of radionuclide concentrations measured in a South African heavy-mineral deposit (de Meijer et al., 1997). One sees the clear difference in concentrations with high K and low Bi and Th values in light minerals and an opposite trend for the heavy minerals. In this example the very high concentrations of Bi and especially Th in monazite becomes apparent. Small monazite admixtures will have a more than proportional impact on the Th concentration in a group of minerals.

The results in this section indicate that there is a clear correlation between the radionuclide concentrations and a mineral. It will be demonstrated that the set of concentrations ( $^{40}\text{K}$ ,  $^{214}\text{Bi}$  and  $^{232}\text{Th}$ ) can be

used to label the mineral or mineral group with a radiometric fingerprint.

### 3. Dating of young dune and beach sediments by thermoluminescence of zircons

Thermoluminescence (TL) is a physical process which is potentially suitable for dating sediments, particularly dune and beach sediments which often do not contain reliable material for radiocarbon dating or are too young or are too difficult to date by other means. The principle of TL can be understood in a simplified band model of an insulator. In the ideal situation all electrons are located in the valence band, separated from the conduction band by an energy gap. Excitation of electrons will bring them temporarily to the conduction band, from which they de-excite to the valence band. In reality the structure of insulators as mineral grains is not perfect and the presence of trace elements, especially of rare earth elements, introduces metastable states, situated between the valence and conduction band. Excitation of the crystal may result in the creation of an electron-hole pair, in which the electron is excited to a metastable state near the conduction band and the hole to metastable state near the valence band. Because these states intercept the electrons and holes for some period of time, they are termed traps.

Exposing the crystals to a temperature excursion will release the trapped electrons. After their release they may be trapped in deeper traps or recombine with a hole. The energy released in this process may be transferred into light. Another way to release electrons from their traps is by irradiating the crystals by light. Usually exposure to daylight for a short period will completely empty the traps. TL dating is based on the assumption that crystals are exposed to daylight before becoming buried in a sediment, removing the TL signal. At the time of burial the traps are therefore empty. Due to exposure to radiation the traps subsequently fill in proportion to the radiation dose rate and the elapsed time. In the laboratory the sample is heated and the light output is measured. The amount of emitted TL light is therefore proportional to the time since burial and dose rate.

Table 1  
Radiometric fingerprint ( $\text{Bq kg}^{-1}$ ) in minerals and mineral associations of heavy-mineral deposit in South Africa

Mineral	$^{40}\text{K}$	$^{214}\text{Bi}$	$^{232}\text{Th}$
Quartz	116 (8)	2 (2)	< 9
Silt/clay minerals	218 (10)	49.4 (1.1)	127 (3)
Ferricrete	95 (7)	130 (3)	160 (4)
Magnetite	< 10	120 (120)	200 (200)
Ilmenite	2.8 (0.5)	18 (2)	27 (9)
Rutile	13 (3)	460 (70)	< 60
Zircon	< 18	3280 (120)	444 (16)
Monazite	1600 (600)	42000 (2000)	181000 (2000)

In various studies TL dating has been applied to sediments buried for long periods of time. Usually quartz crystals have been employed for these experiments and, recently more frequently, feldspar (Mejdahl, 1983; Akber and Prescott, 1985; Strickertsson, 1985) and carbon grains (Debenham, 1982, 1983; Berger and Marshall, 1984; De et al., 1984).

An inherent source of uncertainties is the determination of the integrated radiation dose due to variations in shielding by overlying sediments and radiation absorption by pore water. Using potassium-bearing feldspar, these uncertainties are reduced only slightly because only a small part of the dose is due to the internal  $\beta$ -decay of  $^{40}\text{K}$ . Zircons have received much less attention (see for example Zimmerman, 1979) than quartz and feldspar. In principle, dating with zircons has important advantages due to the high concentrations of U and Th (0.5–0.01%). Because the nuclei in the U and Th decay series emit  $\alpha$ -particles of several MeV and a range which is smaller than the size of the crystals, the dose rate is dominated by the internal radiation and the external conditions can therefore be neglected. Due to the high dose rate, short burial times (about 10–100

years) are measurable. Until now only a few (preliminary) investigations have been reported on TL dating of sediments using zircon due to problems like anomalous fading, resetting, compositional effects like zoning, and grain separation. An important advantage of using zircons for TL dating is that it is commonly present in sand-size detrital material derived from weathering of granites, gneisses and schists. When weathered from such parent rocks its hardness (7.5) enables it to persist in the resulting sediments and hence it is commonly found in many detrital sedimentary environments, including coastal, glacial and fluvial deposits.

At the University of Groningen, in a collaboration between the Department of Solid State Physics and ERG, the Department of Earth Sciences at Utrecht University and the Department of Geology at Florida State University, the feasibility of using zircons as dating material is being investigated. The technique was first applied in a pilot study on zircon-containing sands (Zwanewaterduinen) from the Dutch barrier island of Ameland. These dune sands contain an enhanced concentration of heavy minerals (up to 60%) and zircons constitute about 15% of the mass

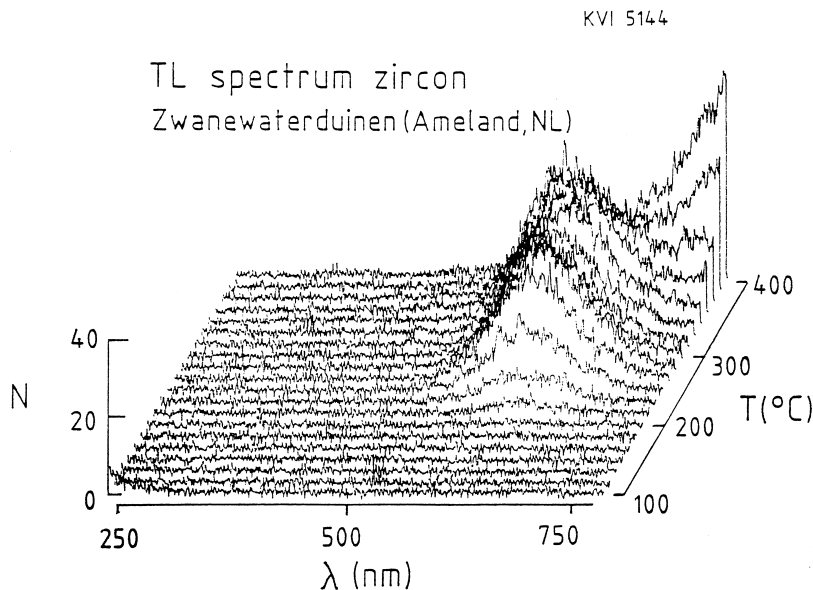


Fig. 5. Natural TL spectrum of a zircon sample from Zwanewaterduinen, Ameland, Netherlands (Hantke, 1991).

of the heavy-mineral suite. Moreover, the age of the dunes is well established from historical records (approximately 1830).

Fig. 5 shows the TL response of zircon samples from Ameland. The emission wavelength is located at 630 nm and shows two maxima at 270° and 350°C. To determine the proportionality factor between the dose received by the sample and the TL response, several heated samples (only empty traps) were exposed to an intense artificial dose with X-radiation. LiF TLDs (thermoluminescent dosimeters) were used to measure the actual dose. In Fig. 6 the resultant TL spectra are shown. Comparison of Fig. 5 and Fig. 6 reveals that the two spectra show similarity in shape and wavelength, suggesting that in the TL processes in these differently treated samples the same recombination centres are involved. The TL runs taken promptly after the artificial irradiation show a signal at temperatures as low as 100°C, whereas the TL response of the natural samples has an onset at about  $T = 200^\circ\text{C}$ . Storage of the X-irradiated samples at 150°C for 1 h removes both the TL

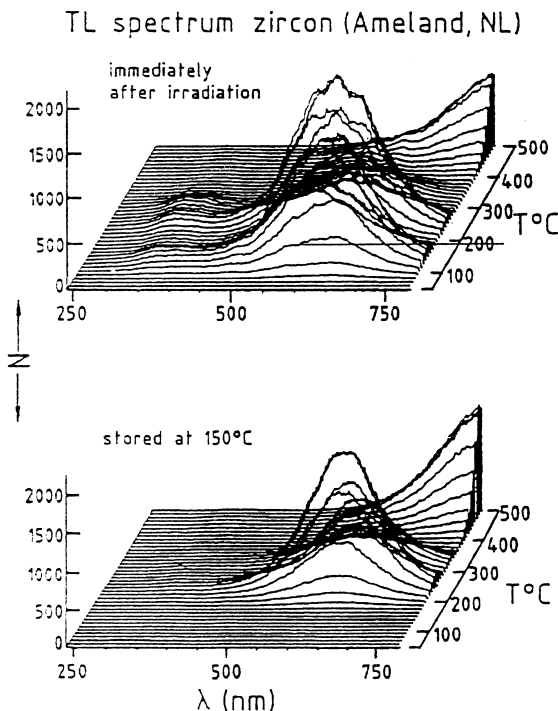


Fig. 6. TL spectrum of X-radiated zircon samples (Zwanewaterduinen), promptly after irradiation (top) and after 1 h storage at 150°C (bottom) (Hantke, 1991).

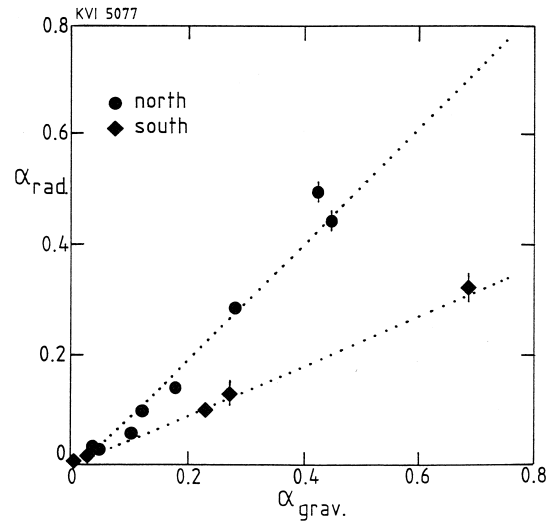


Fig. 7. Comparison of radiometric and gravimetric heavy-mineral mass fractions  $\alpha_{\text{rad}}$  and  $\alpha_{\text{grav}}$ , respectively, in samples of beach sand collected along the Dutch coast. Locations on the mainland are indicated by *SOUTH*, on the islands by *NORTH*. Taken from de Meijer et al. (1990).

response between 100° and 200°C and some minor peaks in the spectral TL distribution near 350 nm (lower part). These excitations are apparently due to emptying of shallow traps (close to the conduction band), which in the natural situation are evidently emptied as fast as they are filled.

Based on the calculated internal (natural) dose rate of  $91 \pm 4 \text{ mGy a}^{-1}$ , the measured TL response for both the naturally radiated and X-irradiated samples and the measured artificial dose, the calculated depositional age of the samples in the Zwanewaterduinen (Fig. 5) is  $160 \pm 40$  years, which is in excellent agreement with the historical date of about 1830 A.D. (Hantke, 1991). The relatively large uncertainty in this result is due to corrections for admixtures in the samples. Using pure zircons would reduce the uncertainty.

The agreement between the TL dating and the historical records does not immediately make zircon a routine tool for dating, but the results indicate that the technique is feasible, and is potentially applicable to samples of young, as well as moderate, geological age. In January 1997 the Dutch organisation 'Stichting voor Technische Wetenschappen' granted funds to develop a reliable and standardised method.

#### 4. Radiometric fingerprinting

Traditionally, the total heavy-mineral content (THM) of sands is determined gravimetrically by floating-off the light minerals in heavy liquids, e.g.,

bromoform. This is an elaborate and tedious procedure. The results in Section 2 indicate a considerable difference in activity concentrations of K, Bi and Th between light and total heavy minerals. The aim of a study conducted by de Meijer et al. (1990) was to

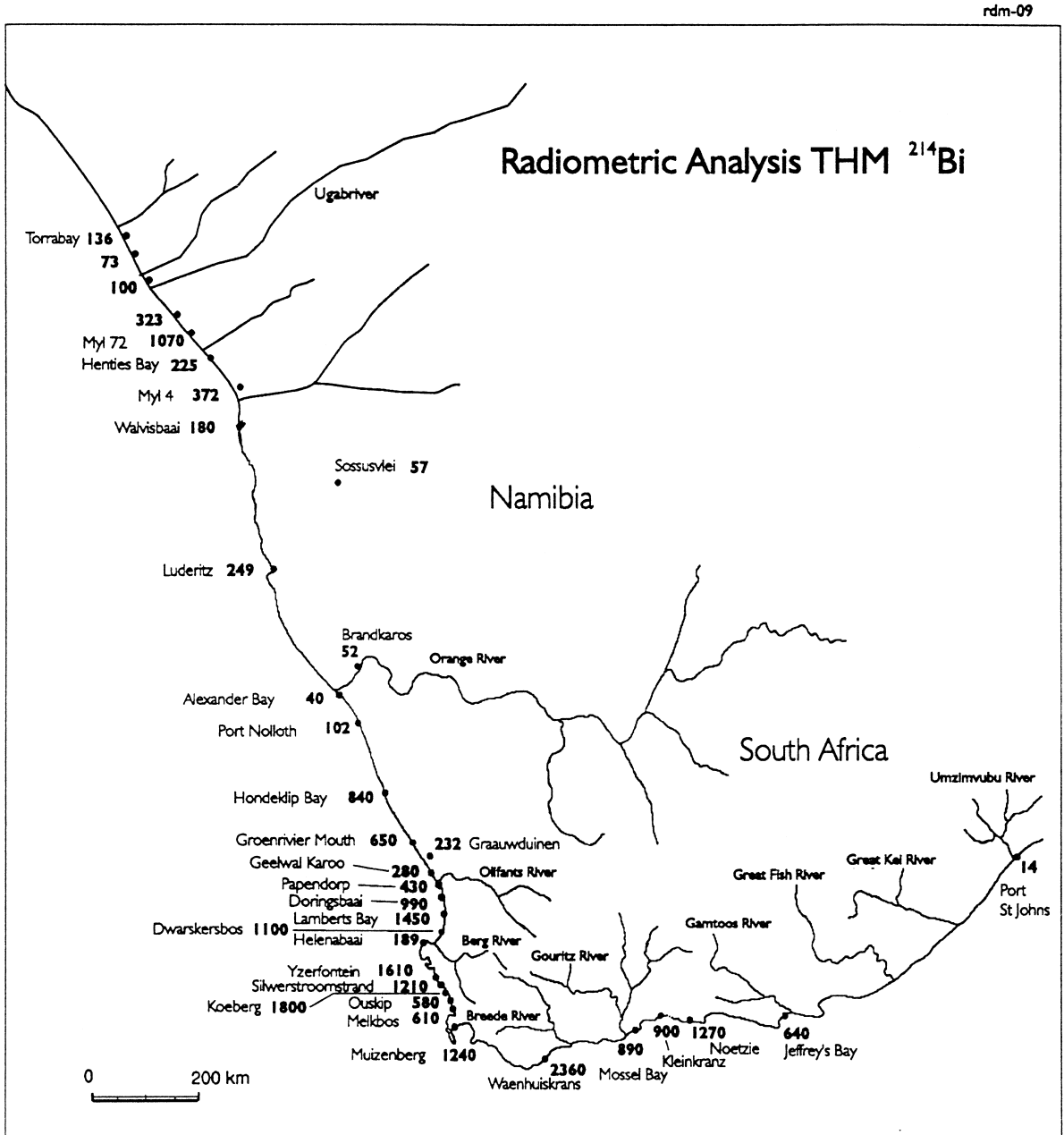


Fig. 8. Activity concentrations (Bq kg<sup>-1</sup>) of  $^{214}\text{Bi}$  in the heavy-mineral fraction of samples sand in South Africa and Namibia.

investigate the possibility of determining the THM value radiometrically from the radiometric fingerprints of the light- and heavy-mineral fractions. If feasible it would open a way to determine THM values fast and in situ.

To test this hypothesis samples of sand collected along the Dutch coast between Scheveningen and Ameland were measured for their natural radionuclide content and split gravimetrically to determine the THM value,  $\alpha_{\text{grav}}$ . The radiometric THM value,  $\alpha_{\text{rad}}$ , for a sample with activity concentrations  $A_i$  was determined from the equation:

$$\alpha_{\text{rad}} = (A_i - A_i^L) / (A_i^H - A_i^L) \quad (1)$$

In this equation the index  $i$  refers to the radionuclide and L and H indicate the light and heavy fraction. The values for  $A_i^L$  and  $A_i^H$  were determined from a sample of sand with a high concentration of heavy minerals taken on the beach (De Hors) of the Dutch Frisian Island of Texel. If the  $A^L$  and  $A^H$  values were universal quantities the values of  $\alpha_{\text{rad}}$  and  $\alpha_{\text{grav}}$  would be identical within the inherent uncertainties. In Fig. 7 the comparison between the two sets of THM values is presented (de Meijer et al., 1990). In the figure two groups of data are present, indicated by NORTH and SOUTH relative to the Texel Inlet Marsdiep.

Because the difference in fingerprint also occurred for the magnetic mineral groups in the sand samples of the De Hors (NORTH) and Bergen (SOUTH), it was concluded that the two groups were not different due to differences in the mineral suite, but due to a difference in origin (provenance) (de Meijer et al., 1990): the southern region corresponds to Rhine deposits, and the northern one most likely to sediments weathered from the Erz Mountains. The latter assignment is based on the fission track ages of individual zircon grains from the NORTH region which fall in the range 225–275 Ma (Andriessen, 1988), consistent with the age of emplacement of granitic rocks in the Erz Mountains.

Subsequent analysis of sediments on the Dutch, German and Danish coast resulted in two additional groups with unique signatures, likely related to glacial deposits (de Meijer and Donoghue, 1995). Transitions between regions are often sharp due to the

effect of tidal inlets. Similar studies have been carried out along the southwest coast of Australia (de Meijer et al., 1998) and the coasts of South Africa and Namibia.

The latter study comprises the largest stretch of coast investigated so far. Fig. 8 shows the  $^{214}\text{Bi}$  concentrations in the bromoform sink (heavy mineral) fraction of the samples. The figure indicates that the Bi values vary over almost two orders of magnitude for this stretch of coast. Regions with similar values are apparent, as are transitions between regions. The regions reflect the mineralogy of the hinterland modified by the effects of river transport and ocean currents. This effect can be observed, for example, in the sediment inputs from the Olifants River and the Orange River, and also in the similarity between the Orange River sediments and the sediments of Port St. John at the Indian Ocean coast. It is conceivable that the majority of both sediments originates in the same area: Drakensbergen. The values for Port St. John and the Orange River are relatively low values. Thus far such values were only noticed at the southwest corner of the Cape Leeuwin Peninsula in western Australia (de Meijer et al., 1998).

Although Fig. 8 shows areas with similar Bi values, there is still considerable variation in mineralogy and radiometry due to influxes of local streams, local coastal outcrops of radionuclide-rich rocks (e.g., Yzerfontein) or variations in mineral composition within the heavy-mineral suite. For a small stretch of the west coast of South Africa, Macdonald et al. (1997), showed that the variations in Bi values are related to the variations in zircon content. These results indicate that it may be more sensible to take the radiometric fingerprint of zircon minerals as an indicator for provenance. An analysis along these lines for the South African and Namibian coasts is presently in progress.

## 5. Mineral composition

The method for determining the THM value radiometrically, as described in Section 4, can be generalized. The radiometric analysis of mineral sand samples yields concentrations of three radionuclides.

In principle, these three concentrations and the fact that the sum of the relative masses is by definition equal to unity, results in four equations from which the relative masses of four groups of minerals may be deduced.

A sample of sand is considered to consist of four mineral groups denoted by subscripts a, b, c and d. Each mineral group,  $i$  ( $i = a, b, c, d$ ) is characterised by its radiometric fingerprint: the three activity concentrations  $C_i(\text{K})$ ,  $C_i(\text{Bi})$  and  $C_i(\text{Th})$ . These three values are the same for all samples and are determined in a calibration procedure (see de Meijer et al., 1997). The samples differ in the relative masses  $m_i$  for each group and in their total activity concentrations  $C^{\text{tot}}(\text{K})$ ,  $C^{\text{tot}}(\text{Bi})$  and  $C^{\text{tot}}(\text{Th})$ . For each sample, therefore, a set of four equations may be set

up in which the four relative masses  $m_i$  are the unknowns

$$\begin{aligned} m_a C_a(\text{K}) + m_b C_b(\text{K}) + m_c C_c(\text{K}) + m_d C_d(\text{K}) &= C^{\text{tot}}(\text{K}) \\ m_a C_a(\text{Bi}) + m_b C_b(\text{Bi}) + m_c C_c(\text{Bi}) + m_d C_d(\text{Bi}) &= C^{\text{tot}}(\text{Bi}) \\ m_a C_a(\text{Th}) + m_b C_b(\text{Th}) + m_c C_c(\text{Th}) + m_d C_d(\text{Th}) &= C^{\text{tot}}(\text{Th}) \\ m_a + m_b + m_c + m_d &= 1 \end{aligned} \quad (2)$$

If more quantities are measured, such as electric conductivity or magnetic susceptibility, the number of equations can be extended and the relative mass of more mineral groups may be deduced. On the other hand, in dealing with heavy minerals only the

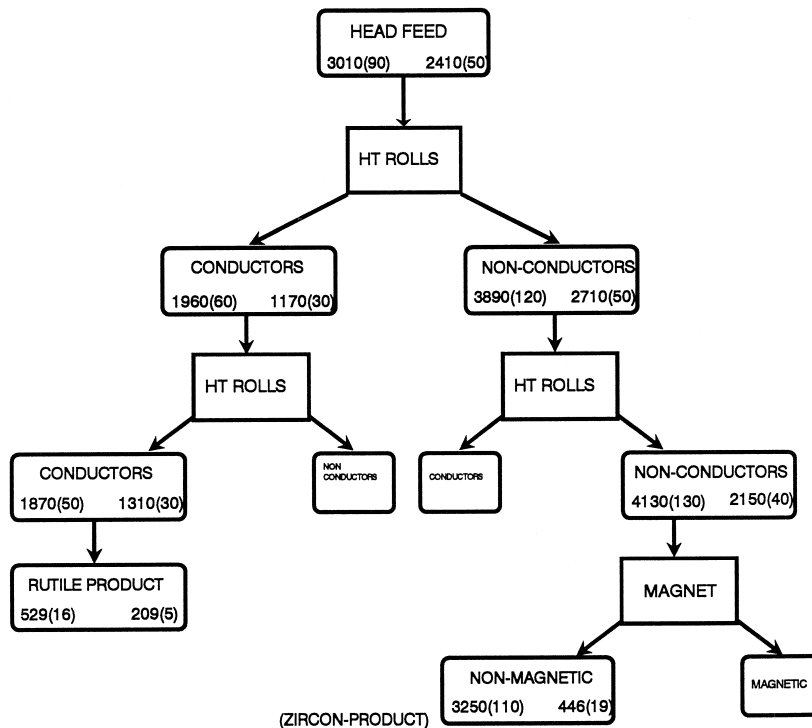


Fig. 9. Schematic representation of various stages in a dry separation unit. The activity concentrations for Bi (left) and Th (right) and their standard deviations are indicated at the bottom of each box.

K content is often small and due to the interference with a Th line in the  $\gamma$ -ray spectrum is known only with large uncertainties. In that case the number of equations and hence the number of groups is reduced to three.

An example of an application of such an analysis is the quality assessment of industrial beneficiation of heavy minerals during various stages of a so-called Dry Mill. Here the heavy minerals arrive after being concentrated in a wet-separation plant. The example presented in Fig. 9 shows the scheme of separation after the magnetic minerals (mainly magnetite and ilmenite) have been removed. In this part of the plant the rutiles and zircons are the main products and their separation is mainly based on electrical conductivity. The figures in the boxes of Fig. 9 represent the Bi (left) and Th activity concentrations with in parentheses the 1 STD uncertainties. The values result from off-line analysis of samples taken at an actual mineral processing plant (de Meijer et al., 1997).

At the high tension (HT) rolls the minerals are fed to a rotating drum. By means of an electrical field induced by a wire at short distance from the roll, the non-conducting minerals become charged. Due to their charge they stick longer to the drum and are rotated over a larger angle than the conducting minerals. A blade separates the two groups. The HT roll separation is subject to humidity variations in the plant.

From Fig. 9 one notes that large changes in activity concentrations can occur at several stages of beneficiation. Measurements of radionuclide concentrations can be carried out on a continuous basis and provide on-line control of the quality of separation. From these measurements, for example, the high voltage on the wire can be adjusted in real-time.

With proper calibration the mineral composition at each stage can also be monitored. As observed in the analysis of the samples, small admixtures of monazite have a large effect on the activity concentrations. Using the values for the activity concentrations in zircon, rutile and monazite, a diagram can be made as presented in Fig. 10. A combination of Bi and Th activity concentrations can be converted to mass percentage of these three nuclides. From such a diagram one may deduce that the high activity concentrations in the 'zircon' line after the second set of

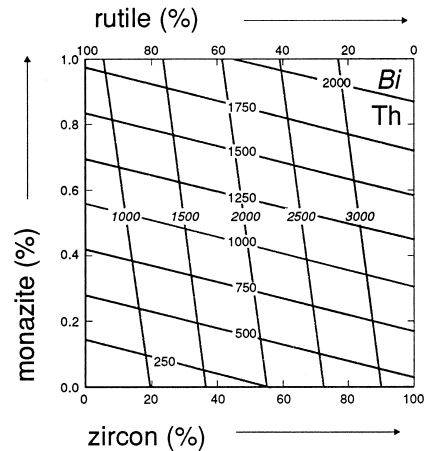


Fig. 10. Diagram indicating Bi and Th activity concentrations ( $\text{Bq kg}^{-1}$ ) and their relation to the mass percentage distribution of zircon, monazite and rutile in mineral mixtures of the dry separation unit. The values are based on the activity concentrations listed in Table 1.

HT ROLLS is due to monazite that is subsequently removed in the MAGNET.

The conductors in the 'zircon'-line and the non-conductors in the 'rutile'-line obtained with the second set of HT ROLLS are fed into the second set of HT ROLLS of the opposite line. In principle minerals can stay in a loop for a long time, consuming considerable energy. A more precise knowledge of the mineral composition at the various stages may help to reduce such losses.

## 6. High-sensitivity $\gamma$ -ray detection

Although not explicitly stated, thus far the radiometric analysis has been carried out in the laboratory. Samples are packed in Marinelli beakers and placed over a hyper-pure germanium detector (HPGe). This detector is placed in a lead shielding to reduce the contribution of natural  $\gamma$ -ray activity from the surrounding building materials. HPGe detectors are known for their high energy resolution, which allows the identification of radionuclides by their  $\gamma$ -ray decay energy. To operate HPGe detectors, they have to be cooled to liquid nitrogen temperatures.

Scintillation crystals in general have a much higher sensitivity to detection of  $\gamma$ -rays than HPGe crystals,

due to their higher density. They are operated at ambient temperatures and are available in larger volumes. Their disadvantage of a poorer energy resolution is not a particular problem in measurements of natural radioactivity (de Meijer et al., 1997). One of the most dense scintillation materials is BGO (Bismuth Germanate) and therefore quite suitable for detection of (high energy)  $\gamma$ -rays emitted in the decay events of  $^{40}\text{K}$  and of the radionuclides in the  $^{238}\text{U}$  and  $^{232}\text{Th}$  decay series. An advantage of the use of scintillation materials such as BGO is the fact that information from the continuum can be included in the analysis of the activity concentrations and mineral composition (see Section 5). This leads to more events per  $\gamma$ -ray detected and improves the efficiency beyond that already arising from the larger volume of the crystal and its greater density. Fig. 11 presents a comparison between HPGe and BGO systems for Bi and Th activity concentrations in a number of samples. The two sets of values agree very well and due to the high sensitivity of the larger BGO crystal, the statistical uncertainties in the BGO data are much lower.

'Standard' spectra for K, Bi and Th and the detector background can be obtained ( $S_{\text{K}}$ ,  $S_{\text{Bi}}$ ,  $S_{\text{Th}}$  and  $S_{\text{B}}$ , respectively). Each of the first three spectra corresponds to the response of the detector in a particular geometry for a sample containing 1 Bq

$\text{kg}^{-1}$  of each nuclide. Each of these spectra, and also the spectrum to be analysed  $S$ , is recorded in  $N$  channels; as a result each spectrum is a series of  $N$  channel contents. The spectrum  $S$  is considered to be a superposition of weighted 'standard' spectra, where the weight factors  $C_{\text{K}}$ ,  $C_{\text{Bi}}$  and  $C_{\text{Th}}$  are the concentrations of each nuclide in the sample:

$$S(i) = C_{\text{K}}S_{\text{K}}(i) + C_{\text{Bi}}S_{\text{Bi}}(i) + C_{\text{Th}}S_{\text{Th}}(i) + S_{\text{B}}(i) \quad (3)$$

The quantities  $C_{\text{K}}$ ,  $C_{\text{Bi}}$  and  $C_{\text{Th}}$  have the same value for channels and are deduced by minimising Eq. (4).

$$Q^2 = \sum_{I=N_{\min}}^{N_{\max}} [S(i) - C_{\text{K}}S_{\text{K}}(i) - C_{\text{Bi}}S_{\text{Bi}}(i) - C_{\text{Th}}S_{\text{Th}}(i) - S_{\text{B}}(i)]^2 / \sigma^2(S(i)) \quad (4)$$

In Eq. (4) the summation ranges over the 'reliable' part of the spectrum, consisting of several hundreds of channels. Therefore there are considerably more equations than unknowns (overdetermined system). The choice of  $N_{\min}$  is strongly influenced by self-absorption effects. This method, based on the deconvolution of the measured spectrum in four standard spectra, is termed 'spectrum deconvolution'.

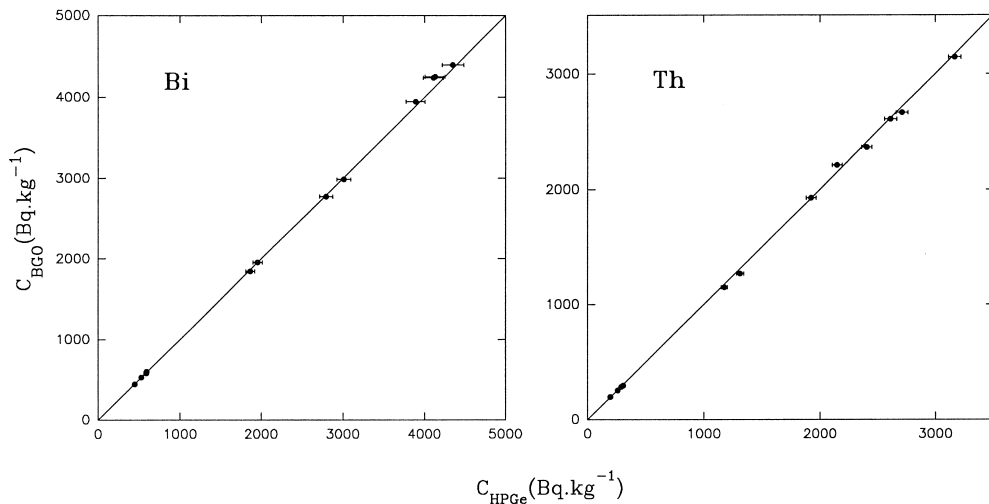


Fig. 11. Comparison of activity concentrations of Bi and Th measured with HPGe and BGO detector systems.

Self-absorption is the absorption of the  $\gamma$ -ray by the material in the sample itself. Self-absorption is stronger for lower energy  $\gamma$ -rays ( $< 300$  keV) and increases strongly with the atomic number  $Z$  of the element. Thus self-absorption is considerably lower in quartz ( $\text{SiO}_2$ ) than rutile ( $\text{TiO}_2$ ) and much lower than in a pure zircon ( $\text{ZrSiO}_4$ ) sample. To avoid systematic uncertainties due to self-absorption effects in heavy-mineral analysis,  $N_{\text{min}}$  was set to correspond to  $E_\gamma = 0.5$  MeV.

'Standard' spectra are obtained by analysing a series of samples with well known concentrations of radionuclides, using the same minimisation procedure leading to Eq. (4). For more details see de Meijer et al. (1997).

## 7. Multi-element detector system for underwater sediment activity (MEDUSA)

Except in the case of heavy-mineral placers, activity concentrations in natural conditions are rather low. Typical values are  $10 \text{ Bq kg}^{-1}$  for  $^{214}\text{Bi}$  or  $^{232}\text{Th}$  and about  $200 \text{ Bq kg}^{-1}$  for  $^{40}\text{K}$ . To be able to map seafloors with a reasonable spatial resolution, measuring times have to be rather short (5 to 10 s). MEDUSA was designed, built, tested and used by the ERG-KVI for in-situ measurements. This system was developed in collaboration with the British Geological Survey (BGS) and contains a number of (modified) components of their 'EEL' system (Miller et al., 1977; Jones, 1994). Besides using a more efficient BGO  $\gamma$ -ray crystal, the MEDUSA system is equipped with a number of sensors such that in addition to seafloor activity concentrations, other information regarding position and sediment characterisation is obtained. The system is internationally patented.

For the present applications either in seafloor mapping, borehole analysis or on-line quality control, the system comprises:

- a number of sensors;
- electronics to amplify, digitise, group and transmit data; and
- a receiving computing unit which derives K, Bi and Th concentrations from a stabilised spectrum using the algorithms described in Section 5. More-

over mineral compositions can be calculated on-line. If the last steps are preferred to be carried out off-line, data are stored.

The latter option is often preferable in the initial stages of an investigation when calibration procedures lead to subsequent refinements in the analysis. Depending on the application, the associated software package is assembled from standardised units.

The BGO detector used in MEDUSA is an order of magnitude more sensitive to Bi and Th measurements than the NaI crystal normally used in the EEL system. The EEL system has shown its potential for seabed  $\gamma$ -ray spectrometry for mineral exploration. For example prospective areas for heavy minerals were delineated in the near-shore zone of Imuruan Bay, off Palawan in the SW Philippines (Ringis et al., 1993). Also, off SW England, granites with uranium vein mineralisation, and uranium anomalies attributed to phosphatic chalk, were mapped (Jones et al., 1988).

### 7.1. Seafloor mapping

One of the practical applications of MEDUSA is radiometric seafloor mapping. In this application the detector system is connected to an armoured coaxial towing cable whose length is adjusted, using a remotely controlled towing winch, to keep the detector in contact with the seabed. The last 30 m of the cable, and the probe containing the sensors is enclosed in a 10 cm diameter PVC hose. The hose protects the probe and cable and prevents it from being snagged by rock outcrops and ship wrecks. Damage to, or loss of, the towed assemblies EEL or MEDUSA, is a very rare event despite more than 20,000 km of towing.

Fig. 12 presents a map of the area of the sea north of the Dutch Frisian Islands of Terschelling and Ameland surveyed in 1994. The map shows the offshore survey lines towed and the Bi + Th activity concentrations as obtained with MEDUSA. The lines are part of a 1 km grid system. The ship's speed was about  $8 \text{ km h}^{-1}$ ; the measuring time 10 s, corresponding to an integrated gamma count over about 20 m of line. The activity concentrations of Bi and Th are often found to be correlated and in this area to be caused by heavy-mineral concentrations. For this area  $\text{THM} = 1\%$  corresponds to about  $15 \text{ Bq}$

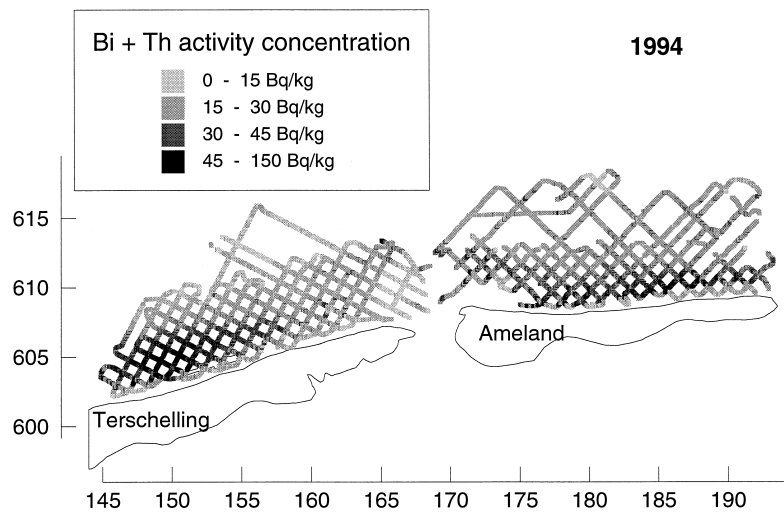


Fig. 12. Map of the seafloor near the Dutch Frisian Islands Ameland and Terschelling. The map shows the contours of the islands and lines towed with the MEDUSA system. The intensity of the lines corresponds to the summed Bi + Th activity concentrations.

$\text{kg}^{-1}$  Bi + Th. The data in Fig. 12 indicate that heavy-mineral concentrations of several percent occur in the near-shore area of both islands. Near Terschelling a large area with THM > 2.5% is present. A more detailed map, in which the data are interpolated, is presented in Fig. 13. From this survey a first-order estimate suggests the presence of about  $0.6 \times 10^6 \text{ m}^3$  of total heavy minerals in a sediment body with more than 2.5% THM. For a

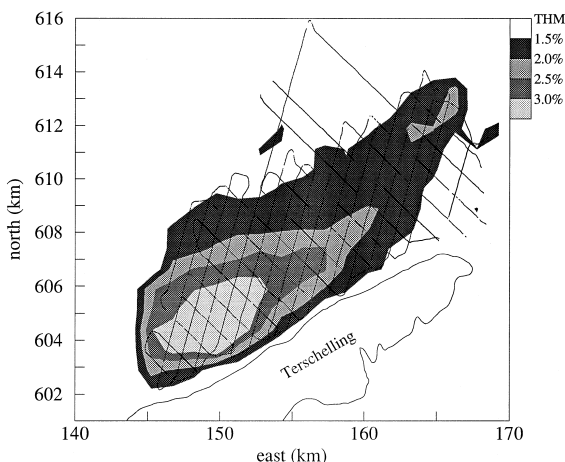


Fig. 13. Detailed map of the surveyed area near Terschelling. The values measured along the lines have been extrapolated and converted to THM values.

number of samples the radiometric and bromoform THM values were measured and found to be in good agreement. The highest concentration found in this area is THM = 20%. Based on these findings, and results and on earlier work near Ameland, mineral companies have applied for exploration concessions for a major part of the Dutch coast.

Near the western part of the surveyed area near Terschelling more detailed studies were carried out in 1995 in the framework of the study on the underwater nourishment Nourtec. The results of this survey, presented in Fig. 14, indicate the existence of sand bars with enhanced Bi and Th concentrations at regular longshore distances and oriented nearly perpendicular to the coast (transverse bars, or so-called saw-tooth bars). Undisturbed sediment cores (up to 40 cm length) revealed enhanced heavy-mineral contents (> 5%) over the full length, providing an indication of the thickness of the deposit.

Fig. 15 presents the results obtained along one of the coast parallel survey lines. In the top part the bathymetry, corrected for tide, is presented. One recognises the sand bars at a regular distance. In the middle part of the figure the total counts of the  $\gamma$ -ray detector are presented. They also show a regular pattern and their peaks correspond to the east part of the bars. The count rate is indicated in cps and because the integrating time is 10 s, a lot of the fine

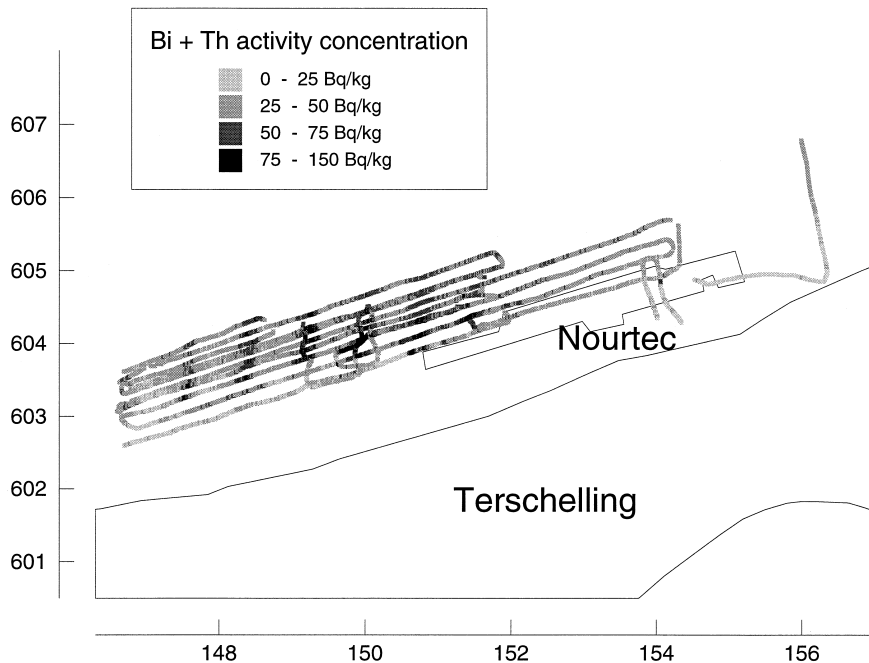


Fig. 14. Map of the area near the underwater nourishment NOURTEC near Terschelling, surveyed with MEDUSA in 1995. The intensity of the lines indicates the summed Bi + Th activity concentrations.

structure is real and not due to statistical fluctuations. In the bottom part the sound level caused by the friction of the protective hose and the sediment is plotted. The sound is recorded by a microphone in MEDUSA and is logarithmically amplified. The sound level is in phase with the troughs of the bar

system. Grab samples revealed no significant difference in grain size between the sediment in the trough and the crest of the bar. It is presently assumed that the noise reflects the bottom roughness and especially the presence of ripple structures on the seabed.

Large variations in these measured values are observed also in directions perpendicular to the coast. Fig. 16 shows a coast perpendicular survey line towed in 1994. This line intersects the nourishment

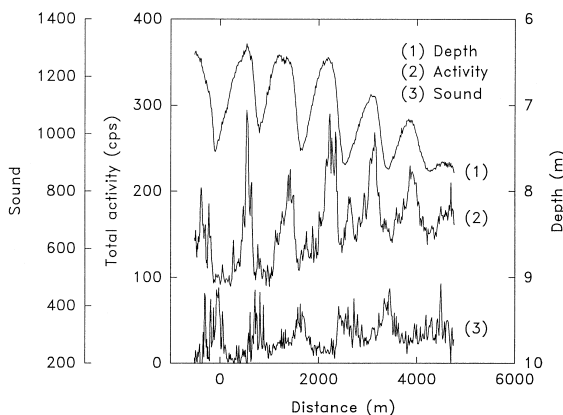


Fig. 15. From top to bottom: bathymetry, total counts and sound level along a coast-parallel survey line. Note the difference in bathymetry and distance scales.

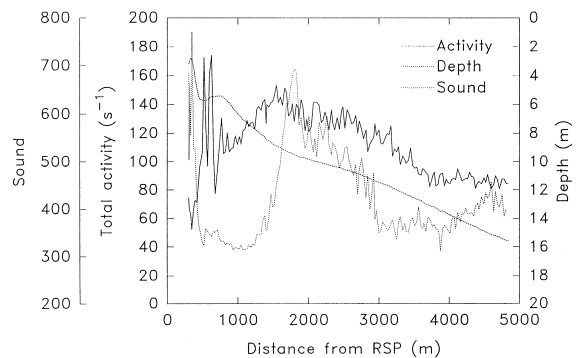


Fig. 16. Cross-shore profiles of bathymetry, total counts and sound level measured near Nourtec, Terschelling in 1994.

area Nourtec where 2.5 million m<sup>3</sup> of sand was added artificially in 1993. The sand used for the nourishment is low in activity concentrations and causes the total counts to have a dip near the nourishment. In the nourishment area, however, a peak in the  $\gamma$ -ray signal is observed. This peak is attributed to a lag deposit formed by the selective removal of light sand after the nourishment. In this figure a remarkable increase in sound level is observed at the convex part in the bathymetry profile. Again this signal is interpreted as a considerable change in bottom roughness. At present two interpretations are offered: either the sound levels are a response to ripple structures because at this depth the near-bottom velocity has dropped from the sheet-flow regime to the ripple regime (A.W. Nideroda, pers. commun., 1996), or the ripples indicate a flow of sediment from the coast to deeper water that occurred during a storm (P. Cowell, Department of Physical Geography, University of Sidney, pers. commun., 1996). These two interpretations are not necessarily in conflict. In both explanations the ripples indicate a type of closure depth, a line where in a certain time frame no net cross-shore transport takes place.

The (friction) sound level data appear to be an interesting quantity, revealing information on seafloor properties. The information is presently more or less qualitative and efforts are being made to make it more quantitative.

## 7.2. Sediment transport

The data presented in the previous subsection indicate that MEDUSA provides synoptical information on various aspects of the seafloor. In this way information over a much larger area is obtained than possible by using in-situ measuring frames, which provide almost continuous information on many quantities at one particular location. The combination of the two types of data should potentially provide a wealth of information on sediment transport. Additionally repeated surveys of certain areas may contribute to a better understanding of large-scale sediment transport processes. Comparison of surveys

along similar grid systems are a potential source of information on sediment volumes transported and transport modes.

The potential inherent in such a method can be appreciated by examination of a set of data taken near Ameland during surveys in 1994 and 1995. In these surveys a similar grid was surveyed with the MEDUSA system. In Fig. 17 maps are presented that show the differences in bathymetry (top), K activity concentration (middle) and Bi + Th (bottom) activity concentration between the 1994 and 1995 surveys. The maps are constructed by interpolating the data obtained along the survey lines by Punctual Kriging techniques (Burgess and Webster, 1980; Davis, 1986), and subsequently determining the difference between the maps over the 1 year interval. In the top part of the figure three areas can roughly be identified:

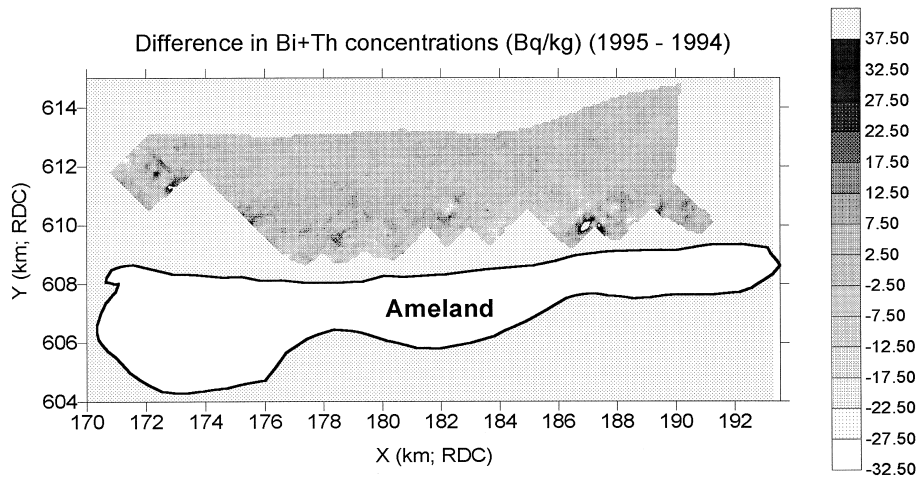
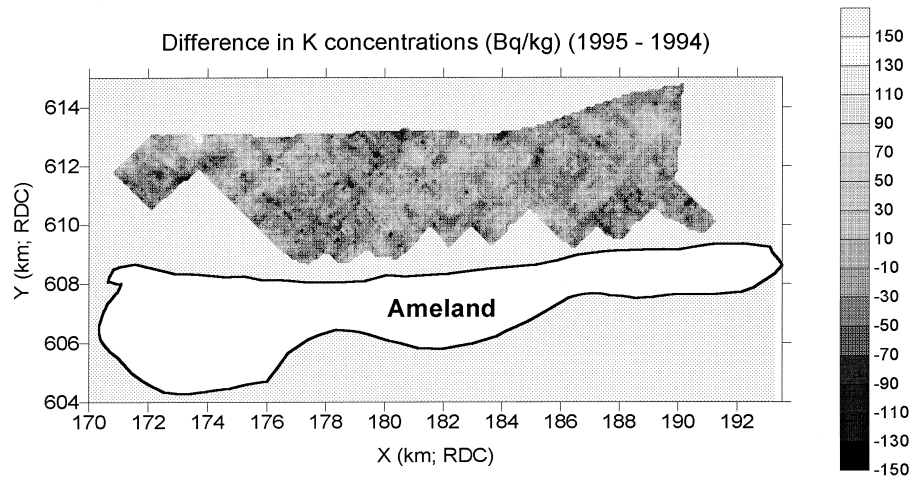
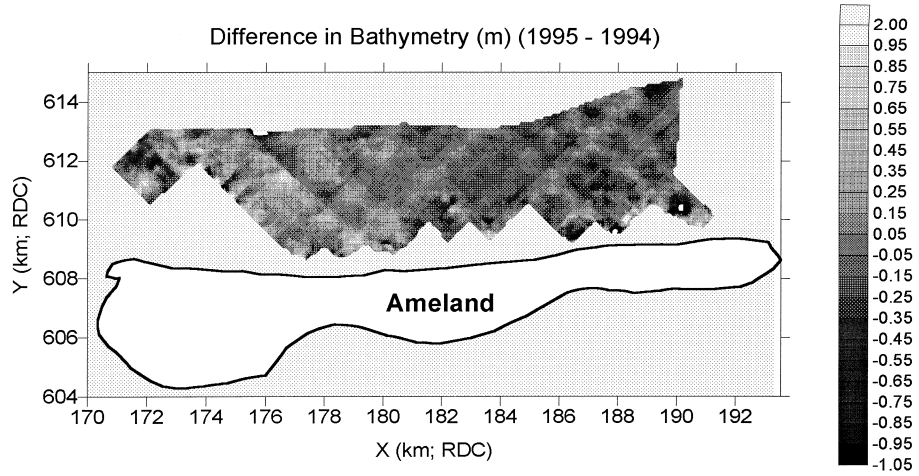
(1) The western part, approximately  $x = 180$  km. In this part sedimentation dominates. Especially along the SE–NW boundary near  $(x, y) = (175, 610)$  alternating erosion and sedimentation patterns occur. This is most likely the area of a migrating (saw-tooth) bar system with a SW–NE orientation. Part of this boundary could be surveyed in 1994 but was too shallow in the 1995 campaign, elucidating the rapid changes taking place in this area. The total change in sediment volume for the area surveyed both in 1994 and 1995 amounts to about 2.5 million m<sup>3</sup>.

(2) The middle part, situated approximately between  $x = 180$  and  $x = 186$  km, is predominantly characterised by erosion (about 1.5 million m<sup>3</sup>).

(3) The eastern part is an area with areas of considerable ( $> 1$  m) erosion as well as sedimentation. These areas mainly occur near the coastline and may indicate migrating bars. The net amount of erosion is 1.7 million m<sup>3</sup>.

The numbers quoted above should be taken with some caution. Bathymetry is determined from the echo sounder of the survey vessel and is corrected for extrapolated tide. The tide range in this area is about  $\pm 2$  m, and including the variations in speed and loading of the vessel, the uncertainty in the difference in bathymetry is about 15 to 25 cm. The

Fig. 17. Map of difference in bathymetry (top), K (middle) and Bi + Th (bottom) activity concentrations between the 1994 and 1995 surveys near Ameland.



surveys were taken over a period of several days and conditions such that the systematic uncertainties obtain a stochastic nature. Hence the accuracy in the quoted amount of transported sediment is larger than expected from the uncertainties in bathymetry. The accuracy is estimated to be about 30%.

Additionally for the changes in K activity concentration, the same three sections as for the bathymetry may be distinguished. In the western part the concentration predominantly diminishes (on average about 24 Bq kg<sup>-1</sup>); in the middle and eastern part the situation is less pronounced, but the dominant trend is a decrease in K content (on average about 14 and 20 Bq kg<sup>-1</sup>, respectively).

In the Bi + Th concentration differences the three areas correspond to a dominant increase, dominant decrease and a 'blotchy' region with increases and decreases, respectively. These tendencies occur mainly near the coastline. In the western part the increase in Bi + Th is accompanied by a sharp decrease in K, the sharp decrease in Bi + Th in the middle part with a moderate increase in K concentration.

The interpretation of the data is made here on the assumption that the two surveys were taken at the appropriate time and spatial scales. It is not a priori clear that this is true for the 1994 and 1995 surveys (it is even likely that this is not the case). Nevertheless to demonstrate the potential of the techniques these uncertainties are ignored. The radiometric information shows that in general the K activity concentration of the sediment at the seafloor is decreasing whilst the Bi + Th concentrations increase. As was shown in Section 2, K is an indicator for light minerals, Bi + Th for heavy minerals. As will be described in Section 9 the work of Tánzos and de Meijer, 1997 in laboratory experiments reveal that the main mode of transport for light minerals is suspension, while for heavy minerals bed load predominates.

In Table 2 the net sediment volume changes and changes in K and Bi + Th activity concentrations are listed. To interpret these data it should be mentioned that on average the K and Bi + Th activity concentrations on the seafloor are about 200 to 300 and 15 to 25 Bq kg<sup>-1</sup>, respectively. Pure heavy minerals near Ameland contain about 1200 Bq kg<sup>-1</sup> Bi + Th and hardly any K. An average decrease of 10 Bq

Table 2

Overview of net sediment volume changes and changes in K and Bi + Th concentrations near the island of Ameland for 1995 relative to 1994

	Unit	Total	West	Middle	East
Area	km <sup>2</sup>	67	27	21	19
Sed. vol.	mm <sup>3</sup>	-0.8	+2.5	-1.5	-1.7
Depth	m	-0.0	+0.1	-0.1	-0.1
K conc	Bq kg <sup>-1</sup>	-20	-24	-14	-20
Bi + Th conc.	Bq kg <sup>-1</sup>	+1.4	+2.4	+0.5	+1.0

kg<sup>-1</sup> K and an increase of about 1 Bq kg<sup>-1</sup> Bi + Th is, in view of the uncertainties, consistent with an overall increase of about 0.1% in THM value of the seafloor sediment. The average content of 1 to 2% THM in the sand near Ameland is considerably higher than for Dutch coastal sands in general (typically about 0.5%). If the observed increase of about 1% in the period 1994–1995 and the enrichment processes are rather continuous processes, the THM values of 1 to 2% indicate an increased erosion rate in the last decades.

## 8. Selective transport studies

### 8.1. Time evolution of beach profiles

In the previous section a comparison was made between quantities in measurements about 1 year apart. One may question whether such a time interval is appropriate in view of the relevant time scales at which processes at the seafloor evolve. Since the access to a beach is easier than of the seafloor, a number of experiments were carried out to assess the time scales and the relation between changes in elevation and changes in radiometry. For that purpose first a number of test sites were studied on the island of Texel (Greenfield et al., 1989). At one of these test sites, where mainly wind action caused transport of sediment, an inverse linear correlation was found between changes in total radioactivity and changes in beach height. This correlation was interpreted as being due to selective transport of light minerals: removal of light minerals increases the concentration of heavy minerals at the surface, whilst

deposition of light minerals has the opposite effect. Donoghue and Greenfield (1991) observed a similar result on beaches of the Gulf of Mexico.

At test sites exposed to both water and wind the correlation was not so simple. Moreover the site disappeared into the sea in time. To further investigate the processes and their time evolution, a larger and more stable site was investigated on the eastern part of the island of Ameland, called Oerd. The site measured  $300 \times 800 \text{ m}^2$  and had a grid size of 25 m. In the period August 1991 till December 1994, 29 measurements were carried out (Tánczos, 1996). Approximately every month elevation (by levelling technique) at each grid point and the total counts of a portable  $\gamma$ -ray meter were measured.

The data were analysed using Empirical Eigenfunction Analysis and resulted in the time and spatial variations of evaluation and radiation level and their correlation. The results indicated that in summer time wind erosion tends to deflate the dry part of the beach, lowering the elevation but increasing the radiation level. The latter is indicative for selective removal of light minerals similar to the results at one of the sites on Texel. In winter time when the beach is inundated regularly the beach is raised and the radiation level drops except at the seaside where a berm of sand is formed with at the top concentrations of heavy minerals. At these locations both the elevation level and the radiation level went up. For more details on the methodology and the results see Tánczos (1996) and references therein.

A beach about 10 km west of the test site sand was nourished and this nourished sand started to erode, the level of the test site showed stepwise an overall increase in height. One should realise that this change in elevation was measured relative to the beach poles, which since 1986 have been subsiding due to the extraction of natural gas. According to measurements by the oil company NAM, the beach subsided 12 to 14 cm in the period 1986 to 1994. The measured relative elevation increase of approximately 7 cm at the test site during the period August 1991 to October 1994 is similar to the measured subsidence of the area and explains why no progradation of the beach was observed.

The stepwise increase of elevation therefore is indicative of a restoration of the natural profile due to the availability of sediment from the nourishment.

The fact that in general sand containing a higher concentration of heavy minerals than the nourished sand is transported onshore indicates that in the transport process of the eroding nourishment, a selection occurs, in which there is a larger net cross-shore transport of heavy minerals than of light minerals. Consequently the light minerals are likely moved eastwards by current-dominated processes. This hypothesis is supported by the seafloor mapping data described in Section 7.2.

## 8.2. Laboratory experiments

In several sections of this paper it was noted that heavy and light minerals were transported differently and that the difference in natural radioactivity allows the observation of the result of the differential transport processes. In itself these observations are not new or surprising, since transport formulae for grains show a dependence on grain size and density. In practice, however, most morphodynamic calculations assume one grain size, usually the  $d_{50}$  value and one density ( $\rho = 2.65 \text{ kg l}^{-1}$ , the density of quartz). To investigate whether selective transport could be observed at all under laboratory conditions and if so, what these studies learn about the processes on the seafloor, a series of experiments with sand enhanced in heavy minerals have been carried out. Of the experiments completed thus far the first one, carried out at near-bottom velocities in the ripple regime and short wave periods, showed that selective transport occurred under all conditions with heavy minerals moving in the direction of the maximum velocity and light minerals either staying in place or moving in the opposite direction (Tánczos, 1996).

In retrospect these observations could qualitatively be explained by taking into account that the velocity to initiate motion for a light mineral grain is lower than for a heavy one. The situation for asymmetric waves is schematically presented in Fig. 18 (de Meijer and Tánczos, 1992). Here the amplitude of the wave is transferred into a horizontal water motion near the seabed according to small-amplitude wave theory. The asymmetric wave is represented by two half-sinuses with different amplitude and wave number. In the schematic case the total water displacement is equal to zero (the areas under the crest and trough are the same). In the crest part of the

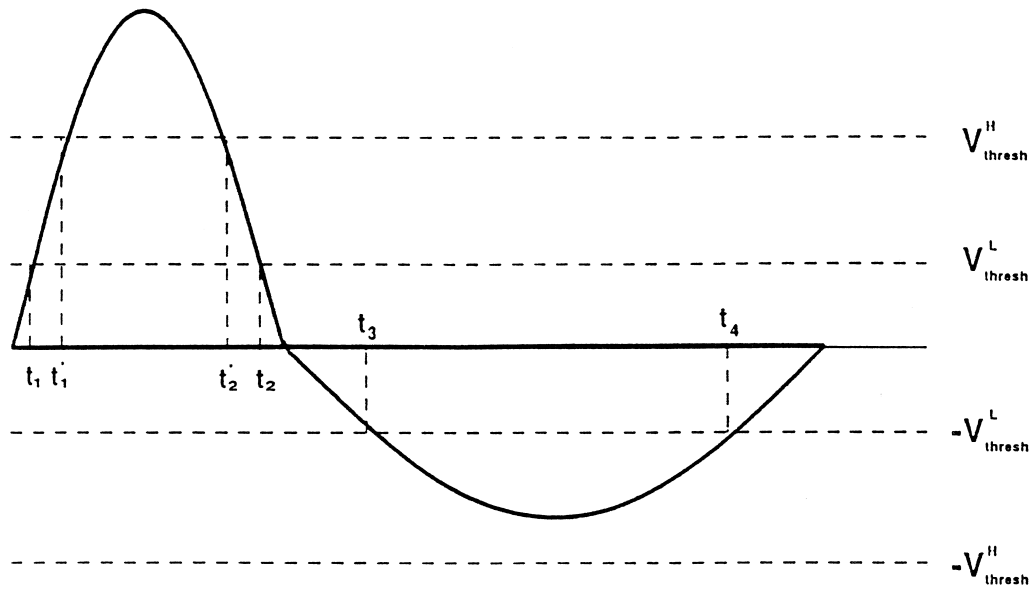


Fig. 18. Schematic presentation of the near-bottom velocity under an asymmetric wave and the threshold velocities for a light and a heavy mineral. Taken from de Meijer and Tánzos (1992).

wave the near-bottom velocities exceed the threshold velocities for both the light and heavy grain, whilst in the trough only the threshold for the light grain is exceeded. This results in a net transport of the heavy grain in the forward direction whereas the light grain shows hardly any net transport.

The above observations and description have led to a simplified physical model to calculate average grain trajectories (Tánzos, 1996; Tánzos and de Meijer, 1997). The results of such a calculation are shown in Fig. 19. The figure shows the difference in behaviour for three types of grain for various values of crest and trough velocities. From the figure one observes that the light minerals under all conditions go into suspension, whilst the heavy ones creep via bed-load transport over the sediment bed. The intermediate grains either creep over the bed or go into suspension depending on the wave conditions.

The second experiment was carried out in the Large Oscillating Wave Tunnel of Delft Hydraulics. These experiments were conducted at longer wave periods and near-bottom velocities in the ripple as well as in the sheet-flow regime. In these experiments the light and heavy minerals move differently, not in opposite directions in this case, but with considerable differences in transport velocities and

modes (light minerals by suspension, heavy minerals by bed-load transport). Moreover it was observed from radiometric measurements that at the surface of the sediment bed the concentration of heavy minerals increased. The increase in this concentration was accompanied by a reduction in the transported volume of sediment. The smaller mobility of the heavy minerals prevented the light ones from being transported, a type of sediment armouring. From the

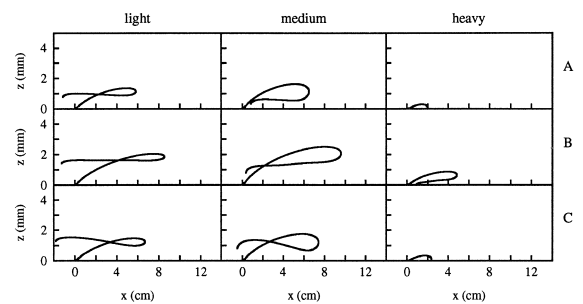


Fig. 19. Calculated average trajectories for three types of grain for various values of the near-bottom velocities under the crest and trough of waves,  $u_c$  and  $u_t$ . (A)  $u_c = 0.5 \text{ m s}^{-1}$ ,  $u_t = 0.3 \text{ m s}^{-1}$ ; (B)  $u_c = 0.6 \text{ m s}^{-1}$ ,  $u_t = 0.3 \text{ m s}^{-1}$ ; (C)  $u_c = 0.5 \text{ m s}^{-1}$ ,  $u_t = 0.4 \text{ m s}^{-1}$ . The thickness of the boundary layer is 5 mm, the effective viscosity coefficient 20. Taken from Tánzos (1996).

changes in radiation intensity an active layer could be derived in which the density of the sediment increases. The thickness of this layer is a few centimetres and corresponds to the darker-coloured layer observed through the glass of the tunnel (Tánczos, 1996).

The results of the calculations with the simplified model mentioned above could be brought into agreement with the data by taking a smaller viscosity coefficient and a greater boundary layer thickness. These changes in value are fortunately in agreement with physical expectations. In the sheet-flow regime ripples have disappeared and hence turbulence is no longer so obvious. Moreover, the longer wave period allows the boundary layer to develop longer and hence the thickness to become larger. The results of these investigations indicate that in addition to grain size and density, the wave parameters—and especially the wave period—play an important role in the transport of sediment. In general the light mineral grains will be transported as suspension load and their transport direction is strongly influenced by currents; heavy minerals stay close to the sediment bed and their transport is wave-dominated. Of course during storm conditions the situation may change such that even heavy minerals will go into suspension. Such conditions could lead to deposition of large amounts of heavy minerals on the beach.

In April 1998 an experiment, carried out in the framework of the European Union research programme 'Marine Science and Technology' (MAST III), has been initiated at the Scheddt Flume at Delft Hydraulics, de Voorst, Netherlands, Germany, where experiments will be carried out without and with addition of heavy minerals. The experiments will be carried out at different wave conditions in a 70 m long, 1.5 m deep and 1 m wide flume in which a beach section is built. The outcome of these experiments will provide answers on the questions related to the transfer of insights obtained in laboratory experiments to actual situations on the seafloor.

## 9. Conclusions and outlook

This paper presents an overview of a multi-disciplinary type of research that originated from a cu-

riosity driven by questions regarding the variability of natural radioactivity. The search for the reasons behind the observed large variabilities required input from a number of scientific disciplines. From nuclear physics was obtained the techniques to measure and to interpret the radioactivity, from solid-state physics came the understanding of defects in crystals and the techniques to interpret the thermoluminescent light, from geochemistry and mineralogy came the techniques to identify the various minerals and the trace elements in them, from geology came the methodology for relating the occurrence of minerals to the parent rocks from which they originate, from sedimentology, morphology and hydrodynamics came the understanding of transport of sand grains and the means for investigating their properties under controlled laboratory conditions. The findings of this multi-disciplinary research are being applied to mineral exploration, mineral processing and coastal engineering and coastal management.

The reason for such a development is likely to be related to the history of nuclear physics. After the discovery of radioactivity by Becquerel just over a century ago, a wide range of applications of radioactivity developed due to its large sensitivity in detection possibilities. The discovery of the neutron and the development of particle accelerators shifted the attention from natural radioactivity to man-made activity which opened a complete new field of science and application. The renewed interest in natural radioactivity allows investigators to 'rediscover' the old field with all new technologies. This renewed interest is partly due to the realisation that the exposure of mankind to radiation is dominated by natural sources including radon, cosmic rays and exposure to  $\gamma$ -radiation from building materials. Even reactor accidents like the one in Chernobyl have, except for the immediate area around the reactor, resulted in a radiation dose which is smaller than the dose to natural sources.

The development of MEDUSA is another example of this trend. The need for larger and more sensitive detectors in nuclear physics has led to the growth of large BGO crystals. In combination with algorithms that allow on-line analysis of the  $\gamma$ -ray spectra in the activity concentrations, software stabilisation of the gain and conversion of radionuclide contents into mineral composition is only possible

with modern soft- and hardware technologies. Similarly, the availability of DGPS and statistical techniques such as Kriging interpolation allow the production of maps that reveal differences of the seafloor properties in time.

The development of techniques will continue, both for those that form the basis of the radiometric techniques and for the application of the radiometry itself. The present detector system is still vulnerable to shocks, because it is photo-multiplier tube based. The development of photo diodes is making progress and smaller crystals can already be mounted on photo diodes. At present the limitations of the photo diodes is their size (about 4 cm<sup>2</sup>) and the noise level at higher (> 50°C) temperatures.

For the present applications the radiometric fingerprinting method needs further development and a stringent test against other methods. It was already experienced that some of the 'standard' techniques are less accurate than often claimed. Intercomparisons will therefore be beneficial for both the radiometry and the 'standard' techniques.

The technique of radiometric fingerprinting is not limited to light and heavy minerals in sand. Presently at ERG the technique is being used to monitor the fate of sludge dumps from Rotterdam harbour into the North Sea and it has been found that sludges can easily be distinguished from sands by fingerprinting techniques. Moreover the sludges seem to be collectors of man-made radioactivity, both from the nuclear industry such as reactors and fuel processing plants and enhanced natural radioactivity released by the non-nuclear industry.

Also the quality control techniques as described in this paper for heavy-mineral processing are likely to be applied in other fields as well. A future application can be seen in the dismantling of nuclear power plants where these techniques may help to separate on-line the concrete debris into low-activity reusable materials and materials that have to be stored as contaminated waste.

To further develop these techniques, two prerequisites have to be fulfilled: one is a multi-disciplinary approach and the other a good link with the developments in fundamental nuclear physics. In this way application of nuclear techniques may remain a gemstone in many sciences.

## Acknowledgements

At the end of this paper, in which the author has focussed on the development of the technique in his own surroundings, he would like to thank all his co-authors in the reference list who have enabled him to work on this topic. A few people I like to thank in particular: Olaf Schuiling for his strong support in the initial phase, Ilka Táncoz for her persistence as the first graduate student on this topic and Joe Donoghue for his geological and sedimentological guidance and his critical reading of the manuscript.

## References

- Akber, R.A., Prescott, J.R., 1985. Thermoluminescence in some feldspars: Early studies of spectra. *Nucl. Tracks* 10, 575–580.
- Andriessen, P.A.M., 1988. Department of Earth Sciences, Free University, Amsterdam. Private communication to R.D. Schuiling.
- Berger, G.W., Marshall, H., 1984. The thermoluminescence of some limestone rocks. *Ancient TL* 2, 1–6.
- Burgess, T.M., Webster, R., 1980. Optimal interpolation and isarithmic mapping of soil properties, I. The semi-variogram and Punctual Kriging. *J. Soil Sci.* 31, 315–331.
- Davis, J.C., 1986. *Statistics and Data Analysis in Geology* (2nd ed.). John Wiley & Sons, New York.
- De, R., Rao, C.N., Kaul, I.K., Sunta, C.M., Nambi, K.S.V., Bapat, V.N., 1984. Thermoluminescence ages of oceanic carbonate sediments: Oozes and chalks from DSDP sites 216, 217, 219 and 220 in the northern Indian Ocean. *Modern Geol.* 8, 207–215.
- de Meijer, R.J., Donoghue, J.F., 1995. Radiometric fingerprinting of sediments on the Dutch German and Danish coasts. *Quat. Int.* 26, 43–47.
- de Meijer, R.J., Táncoz, I.C., 1992. Radiometrisch zandonderzoek. *Ned. Tijdschr. Natuurkd.*, pp. 306–310.
- de Meijer, R.J., Put, L.W., Bergman, R., Landweer, G., Riezebos, H.J., Schuiling, R.D., Scholten, M.J., Veldhuizen, A., 1985. Local variations of outdoor radon concentrations in the Netherlands and physical properties of sand with enhanced natural radioactivity. *Sci. Total Environ.* 45, 101–109.
- de Meijer, R.J., Put, L.W., Schuiling, R.D., de Reus, J.H., Wiersma, J., 1989. Natural radioactivity of heavy minerals in sediments along the Dutch coast. *Proc. KNGMG Symposium 'Coastal Lowlands', Geology and Geotechnology, 1987*, Kluwer, Dordrecht, pp. 355–361.
- de Meijer, R.J., Lesscher, H.M.E., Schuiling, R.D., Elburg, M.E., 1990. Estimate of the heavy mineral content in sand and its provenance by radiometric methods. *Nucl. Geophys.* 4, 455–460.

- de Meijer, R.J., Stapel, C., Jones, D.G., Roberts, P.D., Rozendaal, A., Macdonald, W.G., 1997. Improved and new uses of natural radioactivity in mineral exploration and processing. *Explor. Min. Geol.* 6, 105–117.
- de Meijer, R.J., James, I., Jennings, P.J., Koeyers, J.E., 1998. Radiometric fingerprinting of beach sand in south-western Australia. submitted to *J. Econ. Geol.*
- Debenham, N.C., 1982. Anomalies in the TL of young calcites. *PACT J.* 6, 555–562.
- Debenham, N.C., 1983. Relativity of thermoluminescence dating of stalagmic calcite. *Nature* 304, 154–156.
- Donoghue, J.F., Greenfield, M.B., 1991. Radioactivity of Heavy Mineral Sands as an Indicator of for Coastal Sediment Transport Processes. *J. Coastal Res.* 7, 189–201.
- Greenfield, M.B., de Meijer, R.J., Put, L.W., Wiersma, J., Donoghue, J.F., 1989. Monitoring beach sand transport by use of radiogenic heavy minerals. *Nucl. Geophys.* 3, 231–244.
- Hantke, T.W., 1991. Dating by Thermoluminescence of Young Dune sediments. Master thesis, Univ. of Groningen, Internal Rep. KVI 174/Z-08.
- Jones, D.G., 1994. Towed seabed gamma ray spectrometer: 'Eel' is a radiometric instrument for wide range of offshore mineral exploration, environmental survey applications. *Sea Technol.* August 1994, Compass Publications Inc., Arlington, VA, USA, pp. 89–93.
- Jones, D.G., Miller, J.M., Roberts, P.D., 1988. A seabed radiometric survey of Haig Fras, S. Celtic Sea, U.K. *Proceedings of the Geologist's Association* 99, pp. 193–203.
- Macdonald, W.G., Rozendaal, A., de Meijer, R.J., 1997. Radiometric characteristics of heavy mineral deposits along the west coast of South Africa. *Mineralia Deposita* 32, 371–381.
- Mejdahl, V., 1983. Feldspar inclusion dating of ceramics and burnt stone. *PACT J.* 9, 351–364.
- Miller, J.M., Roberts, P.D., Symons, G.D., Merrill, N.H., Wormald, M.R., 1977. A towed seabed gamma-ray spectrometer for continental shelf surveys. *Nuclear Techniques and Mineral Resources*, IAEA, Vienna, pp. 465–498.
- Ringis, J., Jones, D.G., Roberts, P.D., Caringal, R.R., 1993. Offshore geophysical investigations including use of a sea bed gamma spectrometer, for heavy minerals in Imuruan Bay, NW Palawan, SW Philippines. *Br. Geol. Surv. Tech. Rep.* WC/92/65, 54 pp.
- Schuiling, R.D., de Meijer, R.J., Riezebos, H.J., Scholten, M.J., 1985. Grain-size distribution of different minerals as function of their specific density. *Geol. Mijnbouw* 65, 199–203.
- Strickertsson, K., 1985. The thermoluminescence of potassium feldspars: glow curve characteristics and initial rise measurements. *Nucl. Tracks* 10, 613–617.
- Tánczos, I.C., 1996. Selective Transport Phenomena in Coastal Sands. PhD thesis, Univ. of Groningen, ISBN 90-367-0669-6, 184 pp.
- Tánczos, I.C., de Meijer, R.J., 1997. A semi-quantitative model to calculate grain trajectories for understanding selective transport of heavy and light mineral sands. submitted to *Mar. Geol.*
- Zimmerman, D.W., 1979. Thermoluminescent dating using zircon grains. *PACT J.* 3, 458–465.